ACS OMEGA

Open Access

http://pubs.acs.org/journal/acsodf

Article

Ultrathin Freestanding Nanocellulose Film Prepared from TEMPO-Mediated Oxidation and Homogenized Hydrogel

Tianlei Zhou, Hyung Woo Choi,* and Ghassan Jabbour*

Cite This: *ACS Omega* 2024, 9, 21798−21804

Read Online

ACCESS | Metrics & More | Article Recommendations

ABSTRACT: This paper presents a versatile method to fabricate ultrathin nanofibrillated cellulose (NFC) films as thin as 800 nm by blade coating, which is compatible with a roll-to-roll process on a large scale. Our approach allows obtaining a dried nanocellulose film within a span of 1 h subsequent to 2,2,6,6-tetramethylpiperidine-1-oxyl radical-assisted oxidation and homogenization procedures. One of the thinnest freestanding NFC films with a thickness of 800 nm is achieved using a blade coating of nanocellulose after 72 h of oxidation followed by homogenization with a channel size of 65 μm. Incorporating water-soluble CdTe core-type quantum dots into the nanocellulose film led to a uniform emission under 385 nm UV irradiation, indicating excellent material compatibility. We anticipate nanocellulose developed in our study to be beneficial in biomimicry flying objects, environmentally friendly encapsulation, color filters, and energy storage device membranes, to name a few.

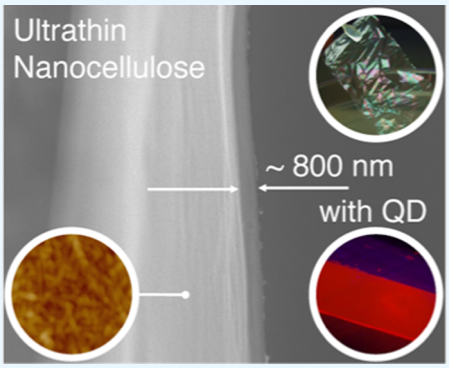

1. INTRODUCTION

Cellulose is regarded as a highly attractive natural substance due to its widespread distribution across the Earth's surface and its significant abundance. Due to its polymerized glucose structure and the presence of numerous intermolecular hydrogen bonds, cellulose exhibits characteristics of both polymer and supramolecular materials. These traits include excellent mechanical strength,[1] flexibility, self-assembly behavior,[2,3] porous structure, and low weight. Currently, it is possible to break down commonly employed cellulose fibers with diameters in the range of several micrometers into nanofibrillated cellulose (NFC) fibers with diameters on the nanometer scale.[4] Consequently, the films composed of nanocellulose demonstrate unique mechanical[5−7] and optical properties[8−10] that are absent in conventional thick cellulose materials. Nanocellulose has a wide spectrum of potential applications, including but not limited to oil absorption,[11] security printing,[12] biological and life science,[13−17] liquid and gas-proof materials,[18−20] water purification,[21] electronic devices,[22−31] and nanocomposites.[25,29,32−37]

Conventional techniques employed for the extraction of NFC from natural cellulose fibers include mechanical methods such as high-pressure homogenization[38,39] and mechanical grinding.[6,40,41] The energy-demanding chemical pretreatment is commonly used to reduce the interaction between cellulose fibers.[42−49] The utilization of 2,2,6,6-tetramethylpiperidine-1-oxyl radical (TEMPO)-mediated oxidation[50] is widely recognized as one of the most effective chemical treatment techniques. This method is favored because it generates a uniform and individualized NFC in a controlled aqueous environment. The TEMPO-mediated oxidation in conjunction with high-pressure homogenization is currently the most popular method for producing high-quality NFC with minimal energy input and high yield.[10,50−53]

Following oxidation-homogenization procedures, the NFC aqueous suspension is typically transformed into thin films to cater to various applications. Vacuum filtering[9,25,36,54] and cast-evaporation[54−56] are the two most common methods for making NFC films. Filtration is deemed more desirable due to its ability to integrate both NFC purification and film creation in a single step, whereas alternative approaches necessitate the initial purification of NFC from chemical salts before subsequent processing can take place. Nevertheless, drawing from our collective expertise, it has been observed that the process of vacuum filtration, employing a 4 L/h oil mechanical pump, necessitates a considerable amount of time to effectively eliminate water and salts. This is true even when a standard filter paper with a relatively high pore size of approximately 25 μm. Additional purification utilizing deionized (DI) water requires a considerable processing time. Incorporating a vacuum pump in filtration procedures increases the power and time consumption, thereby reducing the effectiveness of potential industrial processes. As a result, it is imperative to

Received: October 14, 2023
Revised: March 18, 2024
Accepted: March 21, 2024
Published: May 10, 2024

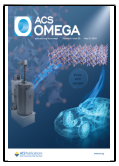

seek an alternative methodology that effectively circumvents the aforementioned limits. In advanced manufacturing of liquid-based thin films and layers, industrial methods like roll-to-roll printing and blade coating are frequently utilized.[57−61]

As of the present, based on our current understanding, the utilization of these methodologies has yielded the production of films derived from cellulose with varying thicknesses ranging from a few micrometers to one hundred micrometers.[6,27] Regarding this matter, the cellulose that was utilized was either produced through solely mechanical processing, without any chemical treatment,[6] or subjected to chemical processes that did not involve aqueous solutions.[27] Given the aforementioned benefits of employing the combined TEMPO-mediated oxidation and mechanical treatment method for the production of NFC liquid suspensions, it is imperative to establish a roll-to-roll compatible procedure for the fabrication of NFC films. Nevertheless, the NFC aqueous suspension obtained from chemical treatment cannot be directly used without first eliminating the salts. Failure to remove the salts leads to the formation of brittle films with crystallized salt regions, thereby impacting both the mechanical capabilities and the optical qualities.

In this study, we demonstrate the use of the blade coating method to create ultrathin freestanding films with a thickness as low as 800 nm utilizing salt-free NFC hydrogel. The NFC hydrogel is acquired by a purification process involving repeated centrifugation and wash steps. In contrast to previous studies,[3,50,62] our approach involves the collection of the solid hydrogel rather than retaining the supernatant. This choice is motivated by several factors: first, the solid hydrogel possesses a high viscosity, which effectively addresses the issue of poor wettability in dilute aqueous solutions. Consequently, it facilitates the formation of a stable and nonshrinkable NFC coating on hydrophobic substrates. Second, the solid NFC hydrogel host promotes improved dispersion of guest materials, thereby minimizing their tendency to aggregate during film production. Lastly, the utilization of the solid hydrogel reduces the drying time of the film due to its lower water content.

2. EXPERIMENTAL SECTION

2.1. Preparation of NFC Suspensions. Figure 1 shows a visual depiction of the NFC hydrogel preparation and simple blade coating process. International Paper supplied the cellulose needed for the NFC film process in the form of Southern bleached softwood kraft (SBSK) paper, as shown in Figure 1. The TEMPO-mediated oxidation process was carried out in accordance with the established methodology described in the literature.[9] At first, 5 g of SBSK was evenly distributed in 500 mL of DI water for 30 min. Next, 0.08 g of TEMPO and 0.5 g of sodium bromide (NaBr) were added to the mixture, which was then supplemented with 35 mL of sodium hypochlorite solution containing 12.5 wt %. The reaction was sustained at a constant pH of 10.5 by continuously adding a 0.5 M NaOH solution during the oxidation process, which lasted either 24 or 72 h at room temperature.

The cellulose aqueous suspensions obtained exhibited stability as a result of considerable electrostatic repulsion between the carboxylated microfibers, which aligns with previous research findings.[50] After undergoing oxidation, the suspensions were homogenized using a microfluidizer (Microfluidics M110) at a pressure of 20,000 psi to create NFC, flowing through channels with either a diameter of 200 or 65 μm. The suspensions exhibited decreased light scattering properties after homogenization, suggesting a prevalence of smaller nanocellulose fibers. By employing lower channel dimensions, the NFC suspensions underwent more homogenization, leading to increased transparency and a more pronounced Tyndall effect, which suggested a decrease in fiber size. The D-labeled aqueous suspension utilizing the channel 65 μm in diameter as well as 72 h of the oxidation process exhibited the greatest transparency and Tyndall effect. This suggests that longer reaction durations result in a higher concentration of carboxylate groups on the surface of the nanocellulose. The NFC aqueous solutions exhibited long-term stability, as no precipitation was seen even after a duration of 2 months.

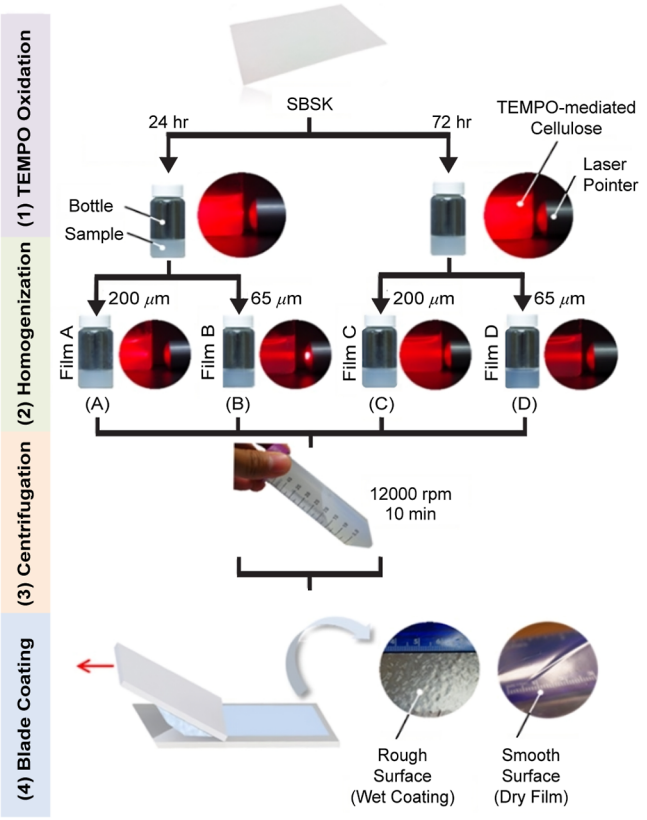

Figure 1. Schematic description of the preparation of the NFC film by blade coating the NFC hydrogel on the PET substrate. The processing approach follows the sequence: (1) TEMPO-mediated oxidation, (2) homogenization, (3) centrifugation, and (4) blade coating. The circle photos shown in (1) and (2) represent the cellulose aqueous suspension exposed to a laser beam as illustrated in the upper right corner. The circle photos shown in (4) represent the rough surface of a wet coating layer and the smooth surface of a peeled dry NFC film.

2.2. Hydrogel and Film Preparation. The formation of the NFC hydrogel required subjecting NFC aqueous suspensions to a centrifugation process, with the purpose of removing remnant salts. After the supernatant was removed, DI water was employed to disperse and wash the NFC hydrogel. Successive centrifugation procedures were performed until the pH of the supernatant reached the target level of 8. The thorough washing process ensured the production of a pure NFC hydrogel, devoid of ionic impurities, which is essential for the formation of high-quality NFC thin films.

https://doi.org/10.1021/acsomega.3c08062
ACS Omega 2024, 9, 21798−21804

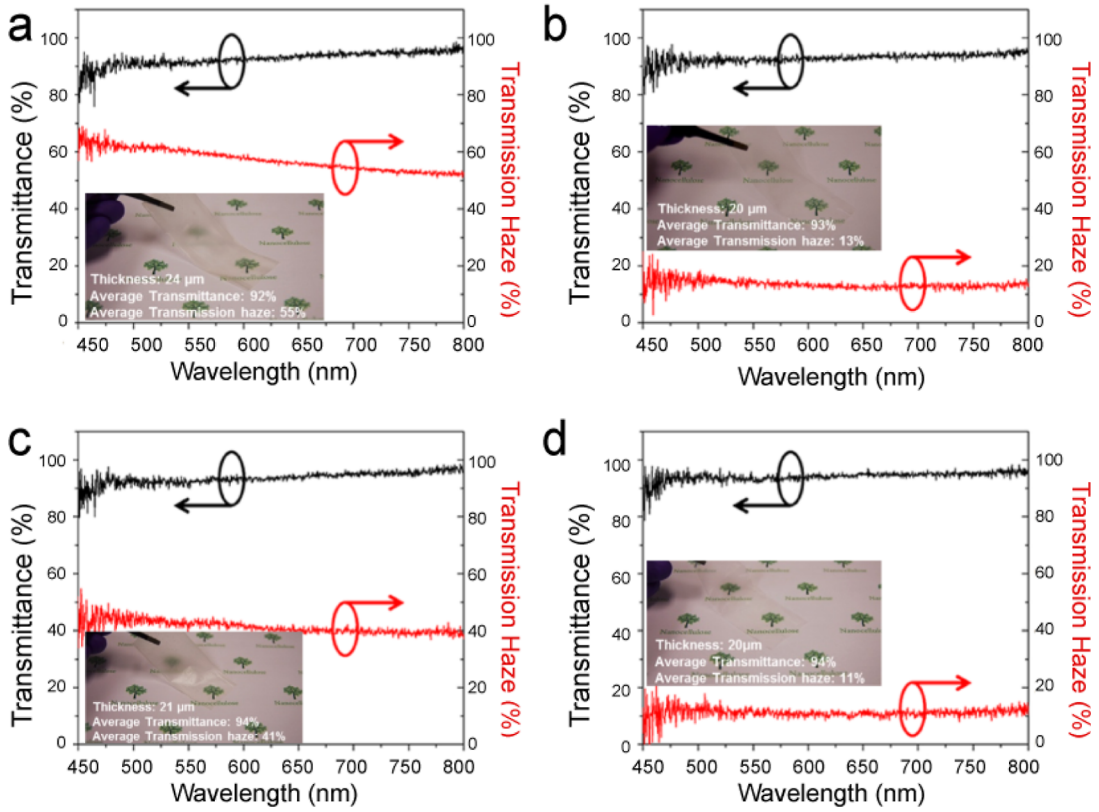

Figure 2. Optical properties of NFC films (a–d) made from NFC treated with different chemical and mechanical processes.

2.3. Nanocellulose Blade Coating. Subsequently, the NFC hydrogel was subjected to a blade coating procedure. The application was performed over a polyethylene terephthalate (PET) substrate, chosen for its hydrophobic characteristics, which made it easier to remove the dried film afterward. The hydrogel was applied by using the roll-to-roll compatible blade coating technique, resulting in a homogeneous layer. The blade coating conditions were optimized to yield dried NFC films with an average thickness of 22 ± 2 μm and 800 ± 150 nm, respectively. This was achieved due to the hydrogel's high viscosity and excellent wetting properties, preventing any shrinking. The coating procedure was devoid of any prerequisite preparation of the PET surface, hence, streamlining the coating fabrication and making it more suitable for a potential industrial manufacturing process. The presence of hydrogen bonding within NFC fibers had a diverse impact on many properties, such as surface tension, wetting behavior, capillary resistance, and viscosity control. This, in turn, resulted in the creation of thin films that were smooth and of superior quality.

2.4. NFC-Quantum Dots Composite Films. To produce quantum dot (QD)-NFC composite films, the blade coating technique was also utilized, along with an extra preliminary step. A solution containing 0.5 mL of CdTe core-type QDs in water was mixed with 15 mL of NFC hydrogel, followed by stirring for 10 min prior to coating. Subsequently, the blend was poured onto a pristine PET surface and uniformly distributed using a glass blade positioned at an angle of roughly 150°. The moist film was dried by exposure to ambient conditions and subsequently removed from the underlying surface using tweezers. The NFC-QD composite films obtained preserved the optical characteristics of the QDs and the structural advantages of NFC. The thickness of composite films was determined using a digital electronic micrometer, except for the 800 nm film, which was verified using field emission scanning electron microscopy (FESEM) analysis, demonstrating the high level of precision in production at the submicron scale.

2.5. Optical Characterization. Quantitative assessment of the optical properties, namely, transmittance and transmission haze, of NFC films was conducted utilizing an optical fiber spectrometer system (Ocean Optics). The equipment set was composed of a spectrometer (USB 2000+), a halogen light source (HL-2000), and an integrating sphere (FOIS-1). The transmittance spectrum was obtained by measuring the intensity of light that passed through the NFC film, which was accurately placed at the entrance port of the integrating sphere using SpectraSuite software. Simultaneously, the transmission haze was assessed by measuring the light intensity as it passed through the NFC film positioned at the exit of the light source. In order to determine the spectrum of scattered light, the data of transmitted light was compared to a reference spectrum obtained without the NFC film in the optical path. This comparison enabled an accurate estimation of the light scattering caused by the film.

3. RESULTS AND DISCUSSION

Figure 2 shows the optical properties of dried films A–D made from NFC aqueous suspensions obtained from various chemical and mechanical treatments, which are described in Figure 1. Transmittance is a metric used to assess the total quantity of light that traverses a substance without being absorbed, whereas transmission haze is a measure that quantifies the extent of scattering or haziness present in the transmitted light. Such optical features have significant

https://doi.org/10.1021/acsomega.3c08062
ACS Omega 2024, 9, 21798–21804

importance in applications that require optical clarity and optimal light transmission characteristics. In the wavelength range 450−800 nm, all films with a thickness of 22 ± 2 μm exhibit a high level of transparency, with transmittance values over 90%, as shown in Figure 2. The observed high optical transmittance can be attributed to the combination of factors including the limited absorption of cellulose within the visible band, smooth layer surface, high purity of the NFC produced by our method, low thickness of the NFC layer, and NFC crystalline size. Moreover, the optical data here points to a uniform distribution of NFC and the formation of a consistent refractive index due to uniform carboxylate groups throughout the film.

Using a homogenization treatment with a 200 μm channel led to a film with an average transmission haze of approximately 55% as shown in Figure 2a. In contrast, Figure 2b showcases a film made by a treatment involving a 65 μm channel, which displays a substantially lower average transmission haze of approximately 13%. The aforementioned statement can also be applied to films subjected to a chemical treatment process lasting 72 h, as depicted in Figure 2c,d. Comparing the films in Figure 2a,c, both of which were produced using NFC treated with a 200 μm homogenization channel, reveals a relatively lower discrepancy of approximately 14% in terms of transmission haze. Figure 2 highlights the influence of oxidation duration and homogenization channel size on the nanocellulose films' optical properties. TEMPO oxidation for 24 h, followed by homogenization through a 200 μm channel, depicted in Figure 2a, results in significant transmission haze due to larger fiber aggregates that scatter light. Conversely, Figure 2b shows reduced haze when utilizing a 65 μm channel for the same oxidation period, indicating finer and more uniformly dispersed fibers, thereby reducing the light scattering. Extended oxidation for 72 h, as in film C (Figure 2c), increases the carboxylate content on the fibers, improving their repulsion and dispersion, which in turn refines the fibrils, yielding a clearer film with less haze compared to the shorter 24 h oxidation in film A (Figure 2a). Although reducing the channel size to 65 μm does improve the optical properties of the nanocellulose film, as shown in Figure 2b, increasing the oxidation period from 24 to 72 h (Figure 2d) in this case does not necessarily lead to a significant improvement in these properties.

Reducing the chamber size for homogenization intensifies the shear forces, which effectively break up the cellulose structure, leading to a decrease in NFC dimensions. Consequently, films homogenized with a narrower chamber size typically display a superior transmittance and transmission haze. However, the data also show that a state of diminishing returns is reached beyond a specific time of oxidation when a lower chamber size is employed for homogenization. This suggests that there might exist an optimal duration for oxidation in order to get the highest level of optical clarity, thus, reducing fabrication costs.

FESEM was employed to confirm and accurately assess the dimensions of NFC and the nanostructure morphology of the films. The findings depicted in Figure 3 demonstrate the presence of a consistent and uniformly arranged assembly of cellulose fibers at the nanoscale. Additionally, FESEM images provide evidence that the size of the fibers in the resulting films is predominantly determined by the dimensions of the homogenizer channel size. On the other hand, the duration of the processing does not have a significant effect on the size

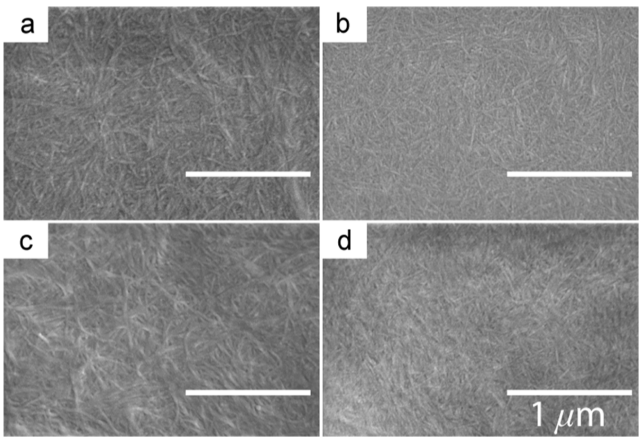

Figure 3. FESEM images of films A (a), B (b), C (c), and D (d). Scale bar is 1 μm.

of the NFC. This observation provides additional support for the association between homogenization treatment and transmission haze, as demonstrated in the films depicted in Figure 2.

NFC hydrogel was used as ink in order to demonstrate the suitability of the blade coating method in the fabrication of a freestanding NFC layer, film (D) (Figure 2d). The wet coating process was tuned in order to achieve a layer thickness of 70 μm. Upon drying, this resulted in the formation of a freestanding thin film with a thickness of 800 ± 150 nm (compared to A4 paper at a thickness of ca. 10^5 nm), as seen by the cross-section view of the FESEM image depicted in Figure 4a. Based on current understanding, our findings

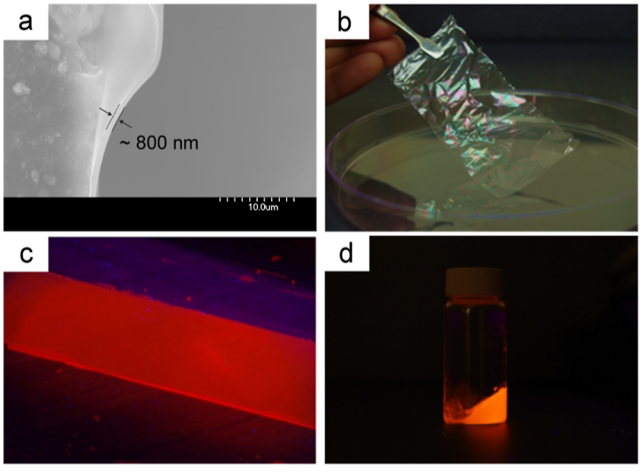

Figure 4. Photos of NFC with QDs. (a) FESEM cross-sectional view of 800 nm-thick NFC film. Scale bar is 10 μm. (b) The NFC film with 800 nm demonstrates a colorful interference pattern. (c) CdTe core-type QDs/NFC composite film under UV light (385 nm). (d) CdTe core-type QDs/NFC hydrogel under UV irradiation after 1 month storage. The hydrogel in the sample bottle was purposely tilted in order to show its stability.

represent the thinnest freestanding blade-coated pure NFC film that has been documented to date. The dried nanocellulose film was peeled off without fracturing, which is attributed to the remarkable mechanical strength of the nanocellulose fibers. The NFC film, in its extremely thin state, might be beneficial in many applications including wing

https://doi.org/10.1021/acsomega.3c08062
ACS Omega 2024, 9, 21798−21804

material for miniature biomimetic flying devices, (ii) decorating materials, (iii) ecofriendly encapsulation, and (iv) membranes for energy storage devices, to mention a few.

Subsequently, water-soluble CdTe core-type QDs were added (0.1 mg/mL) to the NFC hydrogel (24 h, 200 μm) and stirred for 10 min at room temperature, followed by blade coating. Following the water evaporation process, a film exhibiting uniform fluorescence was successfully achieved (see Figure 4c). Homogeneous emission under 385 nm UV irradiation suggests that the QDs were well dispersed throughout the NFC film. The wet composite hydrogel, when stored in a container, exhibited shelf and operational stability for a duration exceeding 1 month. This stability was characterized by the absence of phase separation or aggregation of QDs, as evidenced by the uniform fluorescence emission observed across the entirety of the hydrogel, as depicted in Figure 4d.

4. CONCLUSIONS

In conclusion, a rapid and efficient methodology for fabricating the NFC film has been successfully demonstrated. The utilization of blade coating in conjunction with centrifugation resulted in a notable reduction in the duration required for the manufacture of NFC layers and freestanding ultrathin transparent nanocellulose films.

AUTHOR INFORMATION

Corresponding Authors

Hyung Woo Choi − *Department of Chemical and Materials Engineering, University of Nevada, Reno, Reno, Nevada 89557, United States; School of Electrical Engineering and Computer Science, University of Ottawa, Ottawa, Ontario K1N 6N5, Canada;* orcid.org/0000-0002-5460-5860; Email: hchoi3@uottawa.ca

Ghassan Jabbour − *Department of Chemical and Materials Engineering, University of Nevada, Reno, Reno, Nevada 89557, United States; School of Electrical Engineering and Computer Science, University of Ottawa, Ottawa, Ontario K1N 6N5, Canada*; Email: gja@uottawa.ca

Author

Tianlei Zhou − *Department of Chemical and Materials Engineering, University of Nevada, Reno, Reno, Nevada 89557, United States; Kaneka US Material Research Center (KMR), Kaneka Americas Holding, Inc., Fremont, California 94555, United States*

Complete contact information is available at: https://pubs.acs.org/10.1021/acsomega.3c08062

Author Contributions

The manuscript was written through contributions of all authors. All authors have given approval to the final version of the manuscript.

Notes

The authors declare no competing financial interest.

ACKNOWLEDGMENTS

G.J. acknowledges the support of the Canadian government through the Canada Foundation for Innovation (JELF) Grant, Canada Research Chair (Tier 1) (award # 950-231466), and NSERC Discovery Grant (award # RGPIN- 2020-06970). G.J. acknowledges the support of the University of Nevada, Reno microscopy FESEM facility.

REFERENCES

(1) Zhu, H.; Fang, Z.; Preston, C.; Li, Y.; Hu, L. Transparent Paper: Fabrications, Properties, and Device Applications. *Energy Environ. Sci.* **2014**, *7* (1), 269−287.

(2) Son, H.; Smith, D. M.; Li, Z.; Chang, T.; Xia, W.; Davis, C. S. Particle Alignment Effects on Mechanical Properties of Cellulose Nanocrystal Thin Films. *Mater. Adv.* **2023**, *4* (4), 1053−1061.

(3) Jiang, F.; Hsieh, Y.-L. Chemically and Mechanically Isolated Nanocellulose and Their Self-Assembled Structures. *Carbohydr. Polym.* **2013**, *95* (1), 32−40.

(4) Ahankari, S.; Paliwal, P.; Subhedar, A.; Kargarzadeh, H. Recent Developments in Nanocellulose-Based Aerogels in Thermal Applications: A Review. *ACS Nano* **2021**, *15* (3), 3849−3874.

(5) Yousefi, I.; Zhong, W. A Review of Recent Developments in Nanocellulose-Based Conductive Hydrogels. *Curr. Nanosci.* **2021**, *17* (4), 620−633.

(6) Taniguchi, T.; Okamura, K. New Films Produced from Microfibrillated Natural Fibres. *Polym. Int.* **1998**, *47* (3), 291−294.

(7) Wu, N.; Yang, Y.; Wang, C.; Wu, Q.; Pan, F.; Zhang, R.; Liu, J.; Zeng, Z. Ultrathin Cellulose Nanofiber Assisted Ambient-Pressure-Dried, Ultralight, Mechanically Robust, Multifunctional MXene Aerogels. *Adv. Mater.* **2023**, *35* (1), 2207969.

(8) Jaiswal, A. K.; Hokkanen, A.; Kumar, V.; Mäkelä, T.; Harlin, A.; Orelma, H. Thermoresponsive Nanocellulose Films as an Optical Modulation Device: Proof-of-Concept. *ACS Appl. Mater. Interfaces* **2021**, *13* (21), 25346−25356.

(9) Fang, Z.; Zhu, H.; Yuan, Y.; Ha, D.; Zhu, S.; Preston, C.; Chen, Q.; Li, Y.; Han, X.; Lee, S.; Chen, G.; Li, T.; Munday, J.; Huang, J.; Hu, L. Novel Nanostructured Paper with Ultrahigh Transparency and Ultrahigh Haze for Solar Cells. *Nano Lett.* **2014**, *14* (2), 765−773.

(10) Isogai, A.; Saito, T.; Fukuzumi, H. TEMPO-Oxidized Cellulose Nanofibers. *Nanoscale* **2011**, *3* (1), 71−85.

(11) Korhonen, J. T.; Kettunen, M.; Ras, R. H. A.; Ikkala, O. Hydrophobic Nanocellulose Aerogels as Floating, Sustainable, Reusable, and Recyclable Oil Absorbents. *ACS Appl. Mater. Interfaces* **2011**, *3* (6), 1813−1816.

(12) Chindawong, C.; Johannsmann, D. An Anisotropic Ink Based on Crystalline Nanocellulose: Potential Applications in Security Printing. *J. Appl. Polym. Sci.* **2014**, *131* (22), 41063.

(13) Khakalo, A.; Mäkelä, T.; Johansson, L.-S.; Orelma, H.; Tammelin, T. High-Throughput Tailoring of Nanocellulose Films: From Complex Bio-Based Materials to Defined Multifunctional Architectures. *ACS Appl. Bio Mater.* **2020**, *3* (11), 7428−7438.

(14) Metreveli, G.; Wågberg, L.; Emmoth, E.; Belák, S.; Strømme, M.; Mihranyan, A. A Size-Exclusion Nanocellulose Filter Paper for Virus Removal. *Adv. Healthcare Mater.* **2014**, *3* (10), 1546−1550.

(15) Klemm, D.; Kramer, F.; Moritz, S.; Lindström, T.; Ankerfors, M.; Gray, D.; Dorris, A. Nanocelluloses: A New Family of Nature-Based Materials. *Angew. Chem., Int. Ed.* **2011**, *50* (24), 5438−5466.

(16) Klemm, D.; Schumann, D.; Kramer, F.; Heßler, N.; Koth, D.; Sultanova, B. Nanocellulose Materials - Different Cellulose, Different Functionality. *Macromol. Symp.* **2009**, *280* (1), 60−71.

(17) Yue, X.; Miao, M.; Feng, X. Incorporating of Oxidized Cellulose Nanofibers@d-Limonene Pickering Emulsion into Chitosan for Fully Biobased Coatings toward Fruits Protection. *ACS Sustainable Chem. Eng.* **2023**, *11* (41), 15102−15113.

(18) Aulin, C.; Salazar-Alvarez, G.; Lindström, T. High Strength, Flexible and Transparent Nanofibrillated Cellulose-Nanoclay Biohybrid Films with Tunable Oxygen and Water Vapor Permeability. *Nanoscale* **2012**, *4* (20), 6622.

(19) Österberg, M.; Vartiainen, J.; Lucenius, J.; Hippi, U.; Seppälä, J.; Serimaa, R.; Laine, J. A Fast Method to Produce Strong NFC Films as a Platform for Barrier and Functional Materials. *ACS Appl. Mater. Interfaces* **2013**, *5* (11), 4640−4647.

(20) Teisala, H.; Tuominen, M.; Kuusipalo, J. Superhydrophobic Coatings on Cellulose-Based Materials: Fabrication, Properties, and Applications. *Adv. Mater. Interfaces* **2014**, *1* (1), 1300026.
(21) Farooq, M.; Zou, T.; Riviere, G.; Sipponen, M. H.; Österberg, M. Strong, Ductile, and Waterproof Cellulose Nanofibril Composite Films with Colloidal Lignin Particles. *Biomacromolecules* **2019**, *20* (2), 693−704.
(22) Kang, Y. J.; Chun, S.-J.; Lee, S.-S.; Kim, B.-Y.; Kim, J. H.; Chung, H.; Lee, S.-Y.; Kim, W. All-Solid-State Flexible Supercapacitors Fabricated with Bacterial Nanocellulose Papers, Carbon Nanotubes, and Triblock-Copolymer Ion Gels. *ACS Nano* **2012**, *6* (7), 6400−6406.
(23) Zhu, H.; Xiao, Z.; Liu, D.; Li, Y.; Weadock, N. J.; Fang, Z.; Huang, J.; Hu, L. Biodegradable Transparent Substrates for Flexible Organic-Light-Emitting Diodes. *Energy Environ. Sci.* **2013**, *6* (7), 2105.
(24) Hu, L.; Cui, Y. Energy and Environmental Nanotechnology in Conductive Paper and Textiles. *Energy Environ. Sci.* **2012**, *5* (4), 6423.
(25) Huang, J.; Zhu, H.; Chen, Y.; Preston, C.; Rohrbach, K.; Cumings, J.; Hu, L. Highly Transparent and Flexible Nanopaper Transistors. *ACS Nano* **2013**, *7* (3), 2106−2113.
(26) Hu, L.; Wu, H.; La Mantia, F.; Yang, Y.; Cui, Y. Thin, Flexible Secondary Li-Ion Paper Batteries. *ACS Nano* **2010**, *4* (10), 5843−5848.
(27) Kim, J.; Yun, S.; Mahadeva, S. K.; Yun, K.; Yang, S. Y.; Maniruzzaman, M. Paper Actuators Made with Cellulose and Hybrid Materials. *Sensors* **2010**, *10* (3), 1473−1485.
(28) Zhu, H.; Narakathu, B. B.; Fang, Z.; Tausif Aijazi, A.; Joyce, M.; Atashbar, M.; Hu, L. A Gravure Printed Antenna on Shape-Stable Transparent Nanopaper. *Nanoscale* **2014**, *6* (15), 9110.
(29) Nyström, G.; Razaq, A.; Strømme, M.; Nyholm, L.; Mihranyan, A. Ultrafast All-Polymer Paper-Based Batteries. *Nano Lett.* **2009**, *9* (10), 3635−3639.
(30) Miettunen, K.; Vapaavuori, J.; Tiihonen, A.; Poskela, A.; Lahtinen, P.; Halme, J.; Lund, P. Nanocellulose Aerogel Membranes for Optimal Electrolyte Filling in Dye Solar Cells. *Nano Energy* **2014**, *8*, 95−102.
(31) Zheng, G.; Cui, Y.; Karabulut, E.; Wågberg, L.; Zhu, H.; Hu, L. Nanostructured Paper for Flexible Energy and Electronic Devices. *MRS Bull.* **2013**, *38* (4), 320−325.
(32) Hamedi, M. M.; Hajian, A.; Fall, A. B.; Håkansson, K.; Salajkova, M.; Lundell, F.; Wågberg, L.; Berglund, L. A. Highly Conducting, Strong Nanocomposites Based on Nanocellulose-Assisted Aqueous Dispersions of Single-Wall Carbon Nanotubes. *ACS Nano* **2014**, *8* (3), 2467−2476.
(33) Mihranyan, A.; Esmaeili, M.; Razaq, A.; Alexeichik, D.; Lindström, T. Influence of the Nanocellulose Raw Material Characteristics on the Electrochemical and Mechanical Properties of Conductive Paper Electrodes. *J. Mater. Sci.* **2012**, *47* (10), 4463−4472.
(34) Wu, C.-N.; Yang, Q.; Takeuchi, M.; Saito, T.; Isogai, A. Highly Tough and Transparent Layered Composites of Nanocellulose and Synthetic Silicate. *Nanoscale* **2014**, *6* (1), 392−399.
(35) Koga, H.; Saito, T.; Kitaoka, T.; Nogi, M.; Suganuma, K.; Isogai, A. Transparent, Conductive, and Printable Composites Consisting of TEMPO-Oxidized Nanocellulose and Carbon Nanotube. *Biomacromolecules* **2013**, *14* (4), 1160−1165.
(36) Koga, H.; Nogi, M.; Komoda, N.; Nge, T. T.; Sugahara, T.; Suganuma, K. Uniformly Connected Conductive Networks on Cellulose Nanofiber Paper for Transparent Paper Electronics. *NPG Asia Mater.* **2014**, *6* (3), No. e93.
(37) Jiang, Y.; Zhao, Y.; Feng, X.; Fang, J.; Shi, L. TEMPO-Mediated Oxidized Nanocellulose Incorporating with Its Derivatives of Carbon Dots for Luminescent Hybrid Films. *RSC Adv.* **2016**, *6* (8), 6504−6510.
(38) Herrick, F. W.; Casebier, R. L.; Hamilton, J. K.; Sandberg, K. R. Microfibrillated Cellulose: Morphology and Accessibility. *Journal of Applied Polymer Science: Applied Polymer Symposium*, 1983; Vol 37. no CONF-8205234. https://www.osti.gov/biblio/5039044.
(39) Turbak, A. F.; Snyder, F. W.; Sandberg, K. R. Microfibrillated Cellulose, a New Cellulose Product: Properties, Uses, and Commercial Potential. *Journal of Applied Polymer Science: Applied Polymer Symposium*, 1983; Vol 37; pp 815−827.
(40) Iwamoto, S.; Nakagaito, A. N.; Yano, H.; Nogi, M. Optically Transparent Composites Reinforced with Plant Fiber-Based Nanofibers. *Appl. Phys. A: Mater. Sci. Process.* **2005**, *81* (6), 1109−1112.
(41) Iwamoto, S.; Nakagaito, A. N.; Yano, H. Nano-Fibrillation of Pulp Fibers for the Processing of Transparent Nanocomposites. *Appl. Phys. A: Mater. Sci. Process.* **2007**, *89* (2), 461−466.
(42) Dong, X. M.; Revol, J.-F.; Gray, D. G. Effect of Microcrystallite Preparation Conditions on the Formation of Colloid Crystals of Cellulose. *Cellulose* **1998**, *5* (1), 19−32.
(43) Wågberg, L.; Decher, G.; Norgren, M.; Lindström, T.; Ankerfors, M.; Axnäs, K. The Build-Up of Polyelectrolyte Multilayers of Microfibrillated Cellulose and Cationic Polyelectrolytes. *Langmuir* **2008**, *24* (3), 784−795.
(44) Beck-Candanedo, S.; Roman, M.; Gray, D. G. Effect of Reaction Conditions on the Properties and Behavior of Wood Cellulose Nanocrystal Suspensions. *Biomacromolecules* **2005**, *6* (2), 1048−1054.
(45) Henriksson, M.; Henriksson, G.; Berglund, L. A.; Lindström, T. An Environmentally Friendly Method for Enzyme-Assisted Preparation of Microfibrillated Cellulose (MFC) Nanofibers. *Eur. Polym. J.* **2007**, *43* (8), 3434−3441.
(46) Pääkkö, M.; Ankerfors, M.; Kosonen, H.; Nykänen, A.; Ahola, S.; Österberg, M.; Ruokolainen, J.; Laine, J.; Larsson, P. T.; Ikkala, O.; Lindström, T. Enzymatic Hydrolysis Combined with Mechanical Shearing and High-Pressure Homogenization for Nanoscale Cellulose Fibrils and Strong Gels. *Biomacromolecules* **2007**, *8* (6), 1934−1941.
(47) Marchessault, R. H.; Morehead, F. F.; Walter, N. M. Liquid Crystal Systems from Fibrillar Polysaccharides. *Nature* **1959**, *184* (4686), 632−633.
(48) Van Den Berg, O.; Capadona, J. R.; Weder, C. Preparation of Homogeneous Dispersions of Tunicate Cellulose Whiskers in Organic Solvents. *Biomacromolecules* **2007**, *8* (4), 1353−1357.
(49) Elazzouzi-Hafraoui, S.; Nishiyama, Y.; Putaux, J.-L.; Heux, L.; Dubreuil, F.; Rochas, C. The Shape and Size Distribution of Crystalline Nanoparticles Prepared by Acid Hydrolysis of Native Cellulose. *Biomacromolecules* **2008**, *9* (1), 57−65.
(50) Saito, T.; Nishiyama, Y.; Putaux, J.-L.; Vignon, M.; Isogai, A. Homogeneous Suspensions of Individualized Microfibrils from TEMPO-Catalyzed Oxidation of Native Cellulose. *Biomacromolecules* **2006**, *7* (6), 1687−1691.
(51) Wu, J.; Lin, L. Y. Ultrathin (<1 μm) Substrate-Free Flexible Photodetector on Quantum Dot-Nanocellulose Paper. *Sci. Rep.* **2017**, *7* (1), 43898.
(52) Cao, S.; Liu, P.; Miao, M.; Fang, J.; Feng, X. TEMPO-Oxidized Nanofibrillated Cellulose Assisted Exfoliation of MoS_2/Graphene Composites for Flexible Paper-Anodes. *Chem.—Asian J.* **2022**, *17* (14), No. e202200257.
(53) Miao, M.; Zhao, J.; Feng, X.; Cao, Y.; Cao, S.; Zhao, Y.; Ge, X.; Sun, L.; Shi, L.; Fang, J. Fast Fabrication of Transparent and Multi-Luminescent TEMPO-Oxidized Nanofibrillated Cellulose Nanopaper Functionalized with Lanthanide Complexes. *J. Mater. Chem. C* **2015**, *3* (11), 2511−2517.
(54) Sehaqui, H.; Liu, A.; Zhou, Q.; Berglund, L. A. Fast Preparation Procedure for Large, Flat Cellulose and Cellulose/Inorganic Nanopaper Structures. *Biomacromolecules* **2010**, *11* (9), 2195−2198.
(55) Malainine, M. E.; Mahrouz, M.; Dufresne, A. Thermoplastic Nanocomposites Based on Cellulose Microfibrils from Opuntia Ficus-Indica Parenchyma Cell. *Compos. Sci. Technol.* **2005**, *65* (10), 1520−1526.
(56) Zimmermann, T.; Pöhler, E.; Geiger, T. Cellulose Fibrils for Polymer Reinforcement. *Adv. Eng. Mater.* **2004**, *6* (9), 754−761.
(57) Lee, W.; Koo, H.; Sun, J.; Noh, J.; Kwon, K.-S.; Yeom, C.; Choi, Y.; Chen, K.; Javey, A.; Cho, G. A Fully Roll-to-Roll Gravure-Printed Carbon Nanotube-Based Active Matrix for Multi-Touch Sensors. *Sci. Rep.* **2015**, *5* (1), 17707.

https://doi.org/10.1021/acsomega.3c08062
ACS Omega 2024, 9, 21798−21804

(58) Park, J.; Shin, K.; Lee, C. Roll-to-Roll Coating Technology and Its Applications: A Review. *Int. J. Precis. Eng. Manuf.* **2016**, *17* (4), 537−550.
(59) Keränen, K.; Korhonen, P.; Rekilä, J.; Tapaninen, O.; Happonen, T.; Makkonen, P.; Rönkä, K. Roll-to-Roll Printed and Assembled Large Area LED Lighting Element. *Int. J. Adv. Manuf. Technol.* **2015**, *81* (1−4), 529−536.
(60) Deol, R. S.; Choi, H. W.; Singh, M.; Jabbour, G. E. Printable Displays and Light Sources for Sensor Applications: A Review. *IEEE Sens. J.* **2015**, *15* (6), 3186−3195.
(61) Xiao, Y.; Zuo, C.; Zhong, J.; Wu, W.; Shen, L.; Ding, L. Large-Area Blade-Coated Solar Cells: Advances and Perspectives. *Adv. Energy Mater.* **2021**, *11* (21), 2100378.
(62) Chauhan, P.; Hadad, C.; López, A. H.; Silvestrini, S.; La Parola, V.; Frison, E.; Maggini, M.; Prato, M.; Carofiglio, T. A Nanocellulose-Dye Conjugate for Multi-Format Optical pH-Sensing. *Chem. Commun.* **2014**, *50* (67), 9493−9496.

https://doi.org/10.1021/acsomega.3c08062
ACS Omega 2024, 9, 21798−21804